# Sub-ppb mercury detection in real environmental samples with an improved Rhodamine-based detection system

Sukhdev Singh, Bruno Coulomb, Jean-Luc Boudenne, Damien Bonne, Frédéric Dumur, Bertrand Simon, F. Robert-Peillard

# Sub-ppb mercury detection in real environmental samples with an improved Rhodamine-based detection system

Sukhdev Singh[2], Bruno Coulomb[1], Jean-Luc Boudenne[1], Damien Bonne[2], Frédéric Dumur[3], Bertrand Simon[4], Fabien Robert-Peillard[1]*

[1]Aix Marseille Univ, CNRS, LCE, Marseille, France

[2]Aix Marseille Université, CNRS, Centrale Marseille, iSm2, Marseille, France

[3] Aix Marseille Univ, CNRS, ICR, UMR 7273, F-13397 Marseille France

[4] Institut d'Optique & CNRS, Laboratoire Photonique Numérique et Nanoscience, UMR 5298, Talence, France

*Corresponding author*: fabien.robert-peillard@univ-amu.fr

## Abstract

A new procedure is described for the determination of $Hg^{2+}$ ions in water samples. A Rhodamine based fluorescent sensor was synthesized and the experimental conditions were specifically optimized for application to environmental samples, which requires low detection limits and high selectivity in competitive experiments with realistic concentrations of other metal ions. Incorporation of a Rhodamine-6G fluorophore to a previously described sensor and optimization of the buffer system (detection with acetic acid at pH 5.25) enabled significant enhancement of the sensitivity (detection limit = 0.27 µg.$L^{-1}$) and selectivity. The optimized procedure using high-throughput microplates has been applied to tap and river waters with good results.

**Keywords**: Fluorescent sensor; Mercury ion; Rhodamine derivative; Water analysis.

## 1. Introduction

Mercury is one of the most toxic metals found in the environment, with well-known deleterious effects on kidneys, liver and the central nervous system which leads to various cognitive and

motor disorders [1,2]. Among mercury species, the $Hg^{2+}$ ion has been extensively studied because it can be biomethylated into methyl mercury in the environment [3]. Conventional methods for analysis of mercury in laboratories include cold vapor atomic absorption spectroscopy and inductively coupled plasma mass spectrometry, which are either expensive or complex analytical techniques. Methods based on fluorescent sensors have gained considerable attention in the past years, due to the simplicity of the operations combined to high selectivity and sensitivity of the designed sensors.

Fluorescent sensors based on organic dyes are particularly suited for the analysis of $Hg^{2+}$ ion and other cations [4-6]. This type of sensor includes an ion recognition unit (ionophore) which triggers modification of the fluorescence features of an organic fluorophore. Among these fluorophores, the rhodamine framework has appeared as the ideal choice, due to the high fluorescence quantum yields obtained by the spirolactam cycle opening and the ease of structural modification for the ionophore part. Consequently, several Rhodamine-based molecular sensors for $Hg^{2+}$ have been described in the literature [7].

However, most of these sensors have not convincingly demonstrated their capacities to be applied to the analysis of real environmental waters (tap water, natural waters). To fulfill requirements for these types of analysis, the sensor has to: i) detect mercury in aqueous media; ii) reach high sensitivity with quantification limits below the $\mu g.L^{-1}$ range (the parametric value for the quality of water intended for human consumption in Europe is 1 $\mu g.L^{-1}$ and the maximal allowable concentration in inland waters has been established to 0.05 $\mu g.L^{-1}$ by European Union); iii) prove the selectivity for $Hg^{2+}$ in the presence of very large excess of some other naturally occurring ions (especially $Ca^{2+}$ or $Cu^{2+}$). Regarding application to aqueous sample, rhodamine-based sensors displaying interesting analytical features only in organic or mixed organic-aqueous media will not be efficient [8,9]. Likewise, many sensors have detection limits which are either not indicated or in the $10^{-8}$-$10^{-6}$ M range (2-200 $\mu g.L^{-1}$) [10-12], which is not

enough sensitive for real samples like tap water or natural waters. Selectivity for $Hg^{2+}$ is almost always demonstrated by competitive experiments with 1-10 equivalents of other metal ions compared to mercury [10, 12-16], which is not representative of real environmental samples. Application of Rhodamine fluorescent sensors is thus generally limited to the fluorescence imaging of $Hg^{2+}$ in cells. Only one application to real water samples has been documented by Pan et al. with the determination of $Hg^{2+}$ in industrial wastewaters in the µM range (150-250 $\mu g.L^{-1}$) [17]. Description of a rhodamine sensor designed for tap or natural water analysis is thus highly needed.

Among rhodamine sensors, $NS_2$ ionophore described by Huang et al. [15] seemed particularly suited for aqueous application with high selectivity for $Hg^{2+}$. In the present study we synthesized the rhodamine B sensor (sensor S2, Fig. 1) described by Huang et al. [15]. However, the first experiments using their experimental conditions led us to conclude that the sensitivity seemed too low for application to environmental water samples. We thus decided to modify that sensor by incorporation of a rhodamine-6G fluorophore group (sensor **S1**) and to investigate analytical parameters in order to reach low $\mu g.L^{-1}$ detection limit for application to real water samples. Experiments were performed in microplates to take advantage of the high-throughput screening properties of this type of analytical tool, ideal for optimization purposes. Results of these optimizations are reported in this work.

## 2. Material and methods

### 2.1.Chemicals and reagents

Rhodamine-6G (Dye content: 95%), HEPES (4-(2-Hydroxyethyl)piperazine-1-ethanesulfonic acid), MOPS (3-(N-Morpholino)propanesulfonic acid) and acetic acid were purchased from

Sigma-Aldrich (France). Ultrapure water purified with a Milli-Q system (Millipore, USA, resistivity >18 MΩ cm) was used for the preparations of the whole solutions.

A 1 mg.$L^{-1}$ $Hg^{2+}$ stock solution was prepared daily in a glass vial [18] by dilution of a 1 g.$L^{-1}$ standard solution (AAS grade, Sigma Aldrich) with ultrapure water and a few drops of NaOH 0.1 M solution to set pH of the stock solution between 3.5-4. The same protocol was applied for the other heavy metal stock solutions used for the selectivity study.

5 mM stock solutions of sensors were prepared in DMSO and stored at +4° C (stable for at least 2 months). The stock solution was then diluted in ultrapure water to give a 5 µM working solution (1 ‰ DMSO), which was stable for at least 2 weeks in the fridge.

The tap water sample was collected in the laboratory (Marseille, France). River water samples were collected from the Huveaune (River 1: Roquevaire, France; River 2: Aubagne, France) and the Arc (River 3: Ventabren, France), filtered on 0.45 µm PES filters and stored at +4° C until analysis. pH of the spiked samples was set between 5.2 and 5.3 with diluted $HNO_3$ to avoid pH variation after addition of acetic acid buffer.

## 2.2.Synthesis of sensor **S1** and **S2**

The sensors **S1** was synthesized by a simple modified procedure starting from rhodamine-6G base (**1**) (Scheme 1, see supporting information for detailed procedure). The rhodamine-6G base **1** was reacted with ionophore **NS2** in the presence of 4-toluenesulfonyl chloride (TsCl) and 4-dimethylaminopyridine (DMAP) in dry dichloromethane at room temperature for 4 h and sensor **S1** was obtained in 47% yield as a light pink/beige color solid. $^1$H NMR (400 MHz, $CDCl_3$) δ 8.05-8.00 (m, 1H), 7.62-7.55 (m, 3H), 7.27-7.22 (m, 1H), 7.14 (td, 1H, *J* = 7.6 Hz, 1.4 Hz), 6.84 (td, *J* = 7.7 Hz, 1.7 Hz), 6.34 (d, 2H, *J* = 5.4 Hz), 6.21 (s, 1H), 6.10 (s, 1H), 5.94

(dd, 1H, *J* = 8.0 Hz, 1.4 Hz), 3.53 and 3.45 (2 x s, 2H), 3.34 (d, 1H, *J* = 15.8 Hz), 3.23-3.03 (m, 4H), 2.62 (d, 1H, *J* = 15.7 Hz), 2.48-2.31 (m, 10H), 2.29-2.19 (m, 2H), 1.96 and 1.93 (2 x s, 6H), 1.33-1.22 (m, 6H), 1.15 (t, 6H, *J* = 7.4 Hz). $^{13}$C NMR (100 MHz, $CDCl_3$) δ 166.09, 153.49, 152.93, 151.54, 147.81, 139.80, 133.86, 132.88, 132.80, 129.75, 128.80, 128.70, 128.62, 128.18, 128.12, 126.48, 124.73, 123.61, 120.96, 118.12, 117.19, 108.45, 107.22, 96.88, 96.67, 68.54, 54.52, 54.43, 38.61, 38.49, 30.11, 27.13, 26.22, 17.19, 17.02, 15.01, 14.86. HRMS (EI): Calculated for $C_{41}H_{51}N_4O_2S_2$ $[M+H]^+$ 695.3448; found: 695.3445.

Sensor **S2** was also synthesized using similar procedure as adopted for sensor **S1** starting with rhodamine-base B (**2**) and ionophore **NS2**. With this method, sensor **S2** was obtained as a beige color solid with improved 65% yield as compared to previously reported yield of 26% [15] (see supplementary data for detailed procedure and NMR data).

### 2.3. Instrumentation

Fluorescence spectra of sensor **S1** and sensor **S2** were recorded on a SAFAS Xenius spectrofluorometer (Monaco) equipped with a Xenon lamp and controlled by SP2000 V7 software (SAFAS). Microplate fluorescence measurements were carried out on a microplate reader (Infinite M200, Tecan France SAS, Lyon, France) equipped with an excitation and emission double monochromator (bandwidths of 9 nm and 20 nm for excitation and emission monochromator, respectively) and controlled by i-control™ software (Tecan). Fluorescence detection was performed from above the microplate wells (top configuration), at λex = 540 nm and λem = 575 nm. Operating temperature was set to 25 °C. Other parameters were as follows: gain: 180; number of flashes: 50; integration time: 20 µs. Fluorescence intensities were expressed in arbitrary units (a.u.). Polypropylene black 96 well U-bottom microplates (Nunc), with a maximum capacity of 500 µL for each well were used.

### 2.4. General microplate procedure

300 µL of sample or $Hg^{2+}$ standard solution were dispensed into the wells of the microplate, followed by 50 µL of the buffer solution and 30 µL of the 5 µM working solution of sensor **S1**. The plate was shaken for 3 min in the microplate reader, and fluorescence was subsequently measured at $\lambda_{ex}$ = 540 nm and $\lambda_{em}$ = 575 nm. All experiments were performed in duplicate.

## *3.* **Results and discussion**.

### 3.1. Optimization of experimental conditions

#### 3.1.1. Fluorescence response of **S1** and **S2** at pH 7

The publication from Huang et al. [15] studying **S2** used HEPES buffer at pH 7 (with 15% MeCN). Our first experiments with **S1** and **S2** displayed a negative influence of MeCN on the fluorescent response, so we decided to compare the response of the sensors only in pure aqueous solution. Our analytical protocol used a large volume of sample and addition of a small volume of buffer and sensor, to optimize the analytical performances of the protocol. Standard solutions of 1 $mg.L^{-1}$ $Hg^{2+}$ were neutralized at pH around 4 (starting from stock solution in 5% $HNO_3$) in order to avoid variation of pH between blank and standard solutions. Fluorescence emission spectra recorded on a traditional spectrofluorometer are displayed on Figure 2. As expected, emission wavelength (565 nm) for **S1** with Rhodamine-6G base is lower than **S2** (595 nm) with Rhodamine B base [10]. **S1** also already showed superior performances at low concentrations, with a fluorescence response at 10 $\mu g.L^{-1}$ much better than **S2** (see inset of Fig. 2). We thus decided to focus on the new sensor with Rhodamine-6G for the optimization of the experimental conditions.

#### 3.1.2. Influence of the pH buffer

Most publications study the fluorescence response of the sensors at high concentrations of the metal cation targeted (1-10 µM = 200-2000 µg.$L^{-1}$). Our aim was to develop a simple microplate protocol that could be used at low mercury concentrations more consistent with environmental conditions (linear range up to 10 µg.$L^{-1}$, detection limit below 1 µg.$L^{-1}$), so we first studied the influence of the pH on 10 µg.$L^{-1}$ and 2 µg.$L^{-1}$ standard solutions. High-throughput microplates and a microplate reader were used for all the optimization tests. Results for various pH are presented on Figure 3 (MOPS was used at pH 7 with similar results as HEPES, with better buffer capacity for MOPS than HEPES at pH 7). Interestingly, evolution of the fluorescence response of the sensor is completely different at pH 5.25 compared to pH 7. While ratio between fluorescence response of a 10 µg.$L^{-1}$ and a blank solution is much better at pH 7, results are completely opposite for the 2 µg.$L^{-1}$ standard solution. In fact, only slightly acidic conditions (pH 5-5.5) can enable actual detection of standard solution of $Hg^{2+}$ below 2 µg.$L^{-1}$ with **S1**. Buffers with pH below 5 displayed lower response with both standard solutions.

#### 3.1.3. Influence of the sensor concentration

While better results with low concentration of sensor could be anticipated to improve sensitivity and detection limit [10], our experiments with **S1** did not display a sharp effect when sensor concentration was lowered (Fig. 4). Results were similar in the range 0.5-5 µM but choosing a too low sensor concentration to optimize detection limit could be detrimental for selectivity in presence of other metal cations and both analytical aspects have to be taken into account when one optimize a protocol for application to real environmental samples. We thus decided to keep 5 µM as the optimal concentration value for the rest of the study.

#### 3.1.4. Characterization of the complex between **S1** and $Hg^{2+}$

Regarding stoichiometry of the complex between **S1** and $Hg^{2+}$, the Job's Plot depicted in Figure S1 (for sensor **S1** at pH 5.25) proved the same 1:1 stoichiometry as sensor **S2** at pH 7 [15]. This

was also confirmed by ES(+)-HRMS of a mixture of **S1** and $Hg^{2+}$ (Fig. S9, supplementary data), with a peak at 931.3174 assigned to the single-charged complex $[S1 + Hg^{2+} + Cl^{-}]^{+}$. To further confirm the coordination of Sensor **S1** with $Hg^{2+}$, $^{1}$H-NMR experiments were done. As shown in Figure S10 (supplementary data), the triplet peaks centered at δ1.20 corresponding to methyl groups (1 and 1'), shifted downfield to δ1.41 (Δδ = 0.21 ppm) upon addition of 1 equiv of $Hg^{2+}$ to the sensor **S1**. This shift was attributed to the coordination of sulphur "S" with $Hg^{2+}$. Moreover, the quartets and triplets associated with protons 2, 2', 3 and 3 also shifted to the downfield region of the spectra. The triplets due to the methylene groups attached nitrogen of ionophore part (4 and 4') also shown the shifts towards downfield region of the spectra which indicated the involvement of "N" in coordination with $Hg^{2+}$. The aromatic protons of rhodamine, specially $H_6$, $H_{6'}$, $H_7$ and $H_{7'}$ also shown the clear changes in their chemical shifts due to the shifting of the aromatic bonds (delocalization) that trigger opening of spirolactone upon complexation with $Hg^{2+}$. Based on combined results of NMR and HRMS analysis, we could propose the mode of coordination of sensor **S1** with $Hg^{2+}$ as described in scheme S5 (supplementary data) where both sulphur "S" and "N" of ionophore part, and "O" of carbonyl are involved in the interaction with $Hg^{2+}$.

## 3.2. Analytical performances of sensor **S1**

### 3.2.1. Comparison of the detection limit of **S1** and **S2**

Detection limits for **S1** and **S2** (calculated as $3\sigma_b/s$; $\sigma_b$ is the standard deviation of the blank signals with n=10, and s the slope of the calibration curve) were compared for various experimental conditions (Table 1). The first tests were carried out following the conditions described by Huang et al. for **S2** (with 15% acetonitrile). In our experiments, acetonitrile was not necessary for solubility purposes using the sensor concentration described (25 µL of a 5 µM

sensor solution, corresponding to 0.33 µM in the mixture with sample and buffer; Solutions of **S1** at 5 µM are stable in the fridge at least for 2 weeks after dilution of a 5 mM stock solution in DMSO). At pH 7.1 and 5.25, sensor **S1** could detect mercury at concentrations 3.5 times lower than **S2**, proving that rhodamine-6G base is better than rhodamine B for this type of sensor (Table 1). To the best of our knowledge, this study is the first report which compares the influence of the rhodamine fluorophore (with the same ionophore) on the sensitivity of a sensor.

An excellent detection limit of 0.3 $\mu g.L^{-1}$ (1.5 nM) could be obtained with acetic acid buffer, proving high sensitivity of the new sensor with the optimized experimental parameters. Overall, detection limits using this type of rhodamine sensor have been improved 175 times compared to conditions described before using S2.

| **Experimental conditions** | **S1** | **S2** |
|---|---|---|
| MeCN/HEPES 20 mM pH 7 (15/85)[a] | 19 $\mu g.L^{-1}$ | 53 $\mu g.L^{-1}$ |
| MOPS 50 mM pH 7.1[b] | 2.0 $\mu g.L^{-1}$ | 7.1 $\mu g.L^{-1}$ |
| Acetic acid 50 mM pH 5.25[b] | 0.27 $\mu g.L^{-1}$ | 1.1 $\mu g.L^{-1}$ |

a. In the final mixture; b. Buffer added to the sample (50 µL buffer for 300 µL sample).

Table 1. Detection limits obtained with **S1** and **S2** using different conditions with the microplate protocol. Detection wavelengths for S1: λexc = 535 nm; λem = 570 nm; for S2: λexc = 540 nm; λem = 595 nm.

### 3.2.2. Analytical features for sensor **S1**

The analytical procedure with sensor **S1** was evaluated using the optimized experimental conditions (Table 2). Very good linear regression coefficient was obtained in the range 0.9-20 $\mu g.L^{-1}$ (Fig S2), with excellent RSD value proving repeatability of our measurements. The limit of quantification is below 1 $\mu g.L^{-1}$, which is the parametric value for the quality of water

intended for human consumption in Europe [19]. The protocol can thus be implemented for this kind of samples regarding the European legislation.

| | |
|---|---|
| **Limit of detection (µg.L$^{-1}$)** | 0.27 |
| **Limit of quantification (µg.L$^{-1}$)** | 0.92 |
| **Linear working range (µg.L$^{-1}$)** | 0.9-20 |
| **$R^2$** | 0.997 |
| **RSD (%)[a]** | 2.9 |

a. Calculated on a 5 µg.L$^{-1}$ standard, n= 6 replicates

Table 2. Analytical features of the microplate protocol with **S1**. Buffer: Acetic acid 50 mM pH 5.25.

### 3.2.3. Selectivity study

Selectivity of a sensor for a metal ion is crucial for application to real samples. This is particularly important for mercury ion in environmental samples, with mercury concentration in the nM range, while other metal ions could be present up to a few tens of µM ($Cu^{2+}$, $Zn^{2+}$) or in the mM range ($Ca^{2+}$, $Mg^{2+}$). Most publications describe their selectivity study with µM concentration of $Hg^{2+}$ and 10 equivalents of other metal ion, which are experimental hypothesis clearly not suitable for environmental samples. For this study, we chose $Hg^{2+}$ at 5 µg.L$^{-1}$ (25 nM) in order to obtain a significant response with good repeatability. Concentrations of other metal ions were chosen based on parametric values defined by the European legislation on water intended for human consumption ($Cu^{2+}$, $Pb^{2+}$, $Cd^{2+}$). For metal ions not listed in this legislation, we chose high concentrations that should not be exceeded in a surface water ($Ca^{2+}$, $Mg^{2+}$, $Zn^{2+}$). Response was studied first with each metal ion separately and then under competitive conditions with mercury ion at 5 µg.L$^{-1}$ (Fig. 5). We also compared our optimized experimental

conditions (acetic acid buffer pH 5.25, Fig. 5A) with usual conditions used for this type of sensor (buffer at pH 7, Fig. 5B). The tolerance limit was ± 5% change between the fluorescence of $Hg^{2+}$ alone and the fluorescence in presence of interfering ions at the maximal concentration chosen. Results display excellent selectivity of sensor **S1**, even in competitive experiments with other metal ions in real environmental concentrations (the tolerance limit was not exceeded for all metal ions studied). Interestingly for our study, the same experiment at neutral pH (conditions described by previous group studying sensor **S2**) gives strong interference of copper ions, completely inhibiting response of sensor **S1** with mercury ions. The same results were found with HEPES buffer. pH is thus an important parameter in our procedure to avoid interference from copper ions. Study from Huang et al. with sensor **S2** did not exhibit this interference from copper at pH 7, probably because copper was only five times in excess compared to mercury [15]. We can thus conclude that using realistic metal ions concentrations is clearly necessary to study selectivity and optimize analytical conditions of a new sensor for real life application, especially in the environmental field.

#### 3.2.4. Comparison with other rhodamine sensors

Sensors for mercury detection can be based on rhodamine, fluorescein, coumarin or dansyl organic dyes [5]. Among them, rhodamine sensors gives the best analytical performances, and we thus decided to compare our sensor **S1** with other rhodamine sensors described for applications in aqueous media (Table 3). From this comparison, we can conclude that sensor **S1** is the only sensor for which sensitivity and selectivity have been demonstrated for application to real natural water samples.

| Ref | LOD (µg.L-1) | Selectivity |
|---|---|---|
| 17 | 4.6 | Demonstrated with 1 eq of interferent ions |
| 20 | 14.8 | Interference of $Fe^{3+}$, others demonstrated with 5 eq of interferents ions |
| 21 | 136 | Demonstrated with 30 eq of interferent ions |
| 12 | 470 | Demonstrated with 1 eq of interferent ions |
| 13 | 0.5 | Interference of $Zn^{2+}$, others demonstrated with 5 eq of interferents ions |
| 16 | 0.3 | Demonstrated with 1 eq of interferent ions |
| 10 | 0.6 | Demonstrated with 5 eq of interferent ions |
| This work | 0.27 | Demonstrated with concentration of interferent ions relevant with the analysis of natural water samples (up to 1000 eq for $Cu^{2+}$ and 200.000 eq for $Ca^{2+}$) |

255 Table 3. Comparative study of rhodamine-based sensor for $Hg^{2+}$ analysis in aqueous media.

256

257 3.3. Test with real samples

258 Our optimized protocol was then applied to four real water samples (one tap water and three
259 river samples) to assess the potential of our analytical procedure. Most publications related to
260 mercury sensors describe application to quantify $Hg^{2+}$ levels in living cells, with incubation
261 levels at 20-40 µg.$L^{-1}$ (100-200 nM) [10,11]. Application to environmental samples like natural
262 waters requires lower levels of study. As our selected samples contained no mercury (checked
263 by ICP-MS analysis), samples were spiked at 1 µg.$L^{-1}$ (5 nM) and 2 µg.$L^{-1}$ (10 nM) of mercury.
264 As pH control is important for our protocol (use of an acetic acid buffer at pH 5.25), pH of the
265 real samples was set between 5.2 and 5.3 after spiking. Results for the spiked samples show
266 that good recoveries were achieved (Table 4), demonstrating that our protocol can be applied

to real water samples, even at the µg.L$^{-1}$ level which is the parametric value for the quality of water intended for human consumption in Europe.

| Sample | Spiked concentration of $Hg^{2+}$ (µg.L$^{-1}$) | Found (µg.L$^{-1}$) | Recovery (%) |
|---|---|---|---|
| Tap water | 1 | 0.95 ± 0.11 | 95.0 |
| | 2 | 1.91 ± 0.1 | 95.5 |
| River 1 | 1 | 1.01 ± 0.09 | 101.0 |
| | 2 | 1.88 ± 0.06 | 94.0 |
| River 2 | 1 | 0.88 ± 0.07 | 88.0 |
| | 2 | 1.98 ± 0.06 | 99.0 |
| River 3 | 1 | 0.96 ± 0.1 | 96.0 |
| | 2 | 1.87 ± 0.08 | 93.5 |

Table 4. Detection of $Hg^{2+}$ in spiked real water samples using the microplate protocol. Buffer: Acetic acid 50 mM pH 5.25.

## 4. Conclusions

In conclusion, this study has proven that simple optimizations of a metal ion detection method can result in large enhancement of the analytical performances, required for reliable application to real samples. Replacing rhodamine-B fluorophore by rhodamine-6G on our NS2-containing sensor improved detection limits more than 3-fold. Optimization of the buffer used for detection of $Hg^{2+}$ ion displayed significant effects both on detection limits and selectivity. Acetate buffer

enabled detection of $Hg^{2+}$ below 1 µg.$L^{-1}$ (LOD = 0.3 µg.$L^{-1}$), whereas traditional neutral buffers were limited at 2 µg.$L^{-1}$. Use of acetate buffer also circumvented the problem of copper in competitive experiments, which is a very common issue related to copper as a general fluorescent quencher [22]. The optimized procedure has been successfully applied to real water samples, demonstrating applicability of our new methodology for $Hg^{2+}$ detection.


## Acknowledgements

The project leading to this publication has received funding from the French Research Agency (project « SMART-3D », ANR-18-CE04-0005). Financial support from Aix-Marseille Université, the Centre National de la Recherche Scientifique (CNRS), and Centrale Marseille is also gratefully acknowledged.


## References


[1] C. M. L. Carvalho, E.-H. Chew, S. I. Hashemy, J. Lu, A. Holmgren, Inhibition of the human thioredoxin system, a molecular mechanism of mercury toxicity, J. Biol. Chem. 283 (2008) 11913-11923. https://doi.org/10.1074/jbc.M710133200.

[2] G.Bjørklund, M. Dadar, J. Mutter, J. Aaseth, The toxicology of mercury: Current research and emerging trends, Environ. Res. 159 (2017) 545-554. https://doi.org/10.1016/j.envres.2017.08.051

[3] A. Manceau, M. Enescu, A. Simionovici, M. Lanson, M. Gonzalez-Rey, M. Rovezzi, R. Tucoulou, P. Glatzel, K. L. Nagy, J.-P. Bourdineaud, Chemical forms of mercury in human hair reveal sources of exposure, Environ. Sci. Technol. 50 (2016) 10721-10729. https://doi.org/10.1021/acs.est.6b03468.

[4] T. Rasheed, M. Bilal, F. Nabeel, H. M.N. Iqbal, C. Li, Y. Zhou, Fluorescent sensor based models for the detection of environmentally-related toxic heavy metals, Sci. Total Environ. 615 (2018) 476-485. https://doi.org/10.1016/j.scitotenv.2017.09.126.

[5] N. De Acha, C. Elosúa, J. M. Corres, F. J. Arregui, Fluorescent sensors for the detection of heavy metal ions in aqueous media, Sensors 19 (2019) 599. https://doi.org/10.3390/s19030599.

[6] H. M. Al-Saidi, A. A. El-Bindary, A. Z. El-Sonbati, M. A. Abdel-Fadeel, Fluorescence enhancement of rhodamine B as a tool for the determination of trace and ultra-trace concentrations of bismuth using dispersive liquid–liquid microextraction, RSC Adv. 6 (2016) 21210-21218. https://doi.org/10.1039/c5ra27764g

[7] G. Chen, Z. Guo, G. Zeng, L. Tanga, Fluorescent and colorimetric sensors for environmental mercury detection, Analyst 140 (2015) 5400-5443. https://doi.org/10.1039/c5an00389j.

[8] M. H. Lee, J.-S. Wu, J. W. Lee, J. H. Jung, J. S. Kim, Highly sensitive and selective chemosensor for Hg2+ based on the rhodamine fluorophore, Org. Lett. 9 (2007) 2501-2504. https://doi.org/10.1021/ol0708931.

[9] D. Wu, W. Huang, C. Duan, Z. Lin, Q. Meng, Highly sensitive fluorescent probe for selective detection of Hg2+ in DMF aqueous media, Inorg. Chem 46 (2007) 1538-1540. https://doi.org/10.1021/ic062274e.

[10 ] Y.-J. Gong, X.-B. Zhang, Z. Chen, Y. Yuan, Z. Jin, L. Mei, J. Zhang, W. Tan, G.-L. Shen, R.-Q. Yu, An efficient rhodamine thiospirolactam-based fluorescent probe for detection of $Hg^{2+}$ in aqueous samples, Analyst 137 (2012) 932–938. https://doi.org/10.1039/C2AN15935J

[11] M. De la Cruz-Guzman, A. Aguilar-Aguilar, L. Hernandez-Adame, A. Bañuelos-Frias, F. J Medellín-Rodríguez, G. Palestino, A turn-on fluorescent solid-sensor for Hg(II) detection, Nanoscale Res. Lett. 9 (2014) 1-9. https://doi.org/10.1186/1556-276X-9-431.

[12] M. Li, Y. Sun, L. Dong, Q.-C. Feng, H. Xu, S.-Q. Zang, T. C.W. Mak, Colorimetric recognition of Cu2+ and fluorescent detection of Hg2+ in aqueous media by a dual chemosensor derived from rhodamine B dye with a NS2 receptor, Sens. Actuat. B – Chem. 226 (2016) 332-341. https://doi.org/10.1016/j.snb.2015.11.132.

[13] W. Huang, C. Song, C. He, G. Lv, X. Hu, X. Zhu, C. Duan, Recognition preference of rhodamine-thiospirolactams for Mercury(II) in aqueous solution, Inorg. Chem. 48 (2009) 5061-5072. https://doi.org/10.1021/ic8015657.

[14] W. Lin, X. Cao, Y. Ding, L. Yuan, Q. Yu, A reversible fluorescent Hg2+ chemosensor based on a receptor composed of a thiol atom and an alkene moiety for living cell fluorescence

imaging, Org. Biomol. Chem. 8 (2010) 3618-3620. https://doi.org/10.1039/C0OB00081G.

[15] J. Huang, Y. Xu, X. Qian, A Rhodamine-based Hg2+ sensor with high selectivity and sensitivity in aqueous solution: a NS2-containing receptor, J. Org. Chem. 74 (2009) 2167-2170. https://doi.org/10.1021/jo802297x.

[16] J. Gong, C. Liu, X. Jiao, S. He, L. Zhao and X. Zeng, A novel near-infrared fluorescent probe with improved Stokes shift for specific detection of $Hg^{2+}$ in mitochondria, Org. Biomol. Chem. 18 (2020) 5238-5244. https://doi.org/10.1039/D0OB00507J

[17] F. Pan, J. Mao, Q. Chen, P. Wang, Solid-phase extraction of mercury(II) with magnetic core-shell nanoparticles, followed by its determination with a rhodamine-based fluorescent probe, Microchim. Acta 180 (2013) 1471-1477. https://doi.org/10.1007/s00604-013-1084-6

[18] J. L. Parker, N. S. Bloom, Preservation and storage techniques for low-level aqueous mercury speciation, Sci. Total Environ. 337 (2005) 253-263. https://doi.org/10.1016/j.scitotenv.2004.07.006

[19] ANNEXES to the Proposal for a Directive of the European Parliament and of the Council on the quality of water intended for human consumption (recast), European Commission, COM(2017) 753 final 2017/0332.

https://eur-lex.europa.eu/resource.html?uri=cellar:8c5065b2-074f-11e8-b8f5-01aa75ed71a1.0016.02/DOC_2&format=PDF

[20] F. Yan, D. Cao, M. Wang, N. Yang, Q. Yu, L. Dai, L. Chen, A New Rhodamine-Based "Off-On" Fluorescent Chemosensor for Hg (II) Ion and its Application in Imaging Hg (II) in Living Cells, J. Fluoresc. 22 (2012) 1249-1256. https://doi.org/10.1007/s10895-012-1065-x

[21] X. Li, R. Zhao, Y. Wei, D. Yang, Z. Zhou, J. Zhang, Y. Zhou, A rhodamine derivative for $Hg^{2+}$-selective colorimetric and fluorescent sensing and its application to in vivo imaging, Chin. Chem. Lett. 27 (2016) 813-816. https://doi.org/10.1016/j.cclet.2016.04.001

[22] S. Mizukami, T. Nagano, Y. Urano, A. Odani, K. Kikuchi, A fluorescent anion sensor that works in neutral aqueous solution for bioanalytical application, J. Am. Chem. Soc. 124 (2002) 3920-3925. https://doi.org/10.1021/ja0175643.

## Figure captions

*Figure 1. Structure of sensors **S1** and **S2**.*

*Figure 2- Fluorescence emission spectra of sensors **S1** and **S2** in the presence of different concentrations of $Hg^{2+}$. Excitation was performed at 535 nm. Protocol: 1 mL sample + 150 µL HEPES buffer 50 mM pH 7.0 + 100 µL sensor 5 µM, shaking for 3 min. Inset: Zoom for fluorescence intensity between 0 and 10.*

*Figure 3- Comparison of the response of **S1** with two standard solutions, depending on the buffer. Microplate protocol. Buffer: Acetic acid 50 mM for pH 5-5.5; MES 50 mM for pH 6-6.5; MOPS 50 mM for pH 7-8. (A) Fluorescence intensities; (B) Ratio of fluorescence intensities between standard solutions and blank (F2/F0: ratio Hg 2 $\mu g.L^{-1}$/blank; F10/F0: ratio Hg 10 $\mu g.L^{-1}$/blank).*

*Figure 4- Influence of the sensor **S1** concentration on the fluorescence response. Microplate protocol. Sensor concentration is the concentration in the 25 µL of sensor added to the sample. Buffer: Acetic acid 50 mM pH 5.25. $F_5/F_0$ is the ratio between the fluorescence response of a 5 $\mu g.L^{-1}$ standard solution and the blank.*

*Figure 5. Selectivity study with sensor **S1**. A. Buffer: Acetic acid 50 mM pH 5.25. B: Buffer: MOPS 50 mM pH 7.1. Microplate protocol, $F/F_0$ is the ratio between the fluorescence response of the metal ions solution and the blank.*

*Scheme 1. Synthesis of Sensor **S1***

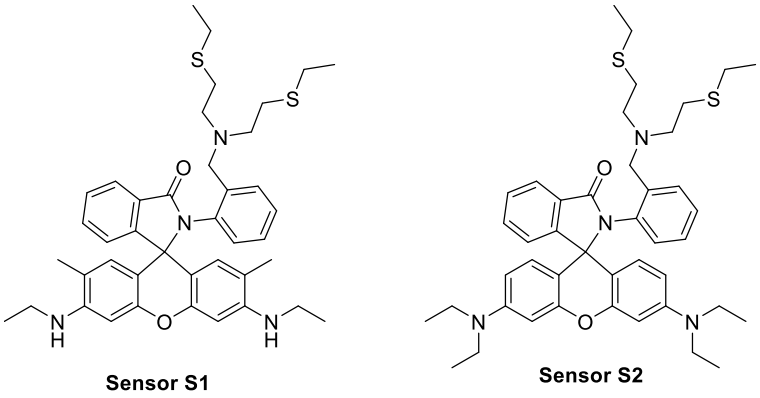


**Figure 1**. Structure of sensors **S1** and **S2**

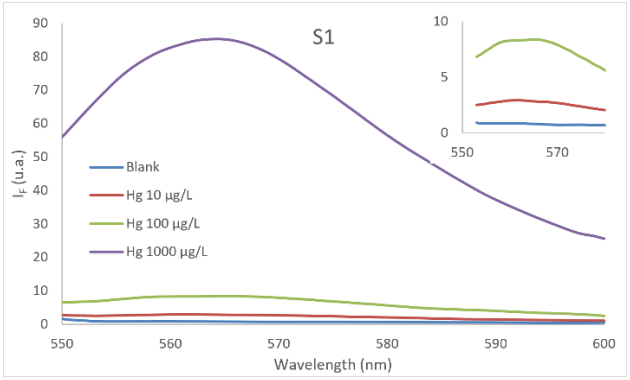


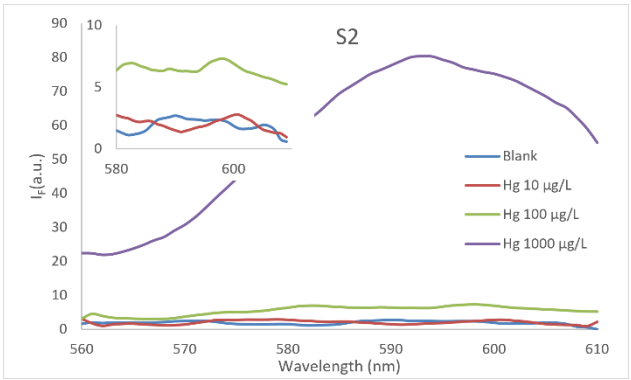


**Figure 2.** Fluorescence emission spectra of sensors **S1** and **S2** in the presence of different concentrations of $Hg^{2+}$. Excitation was performed at 535 nm. Protocol: 1 mL sample + 150 µL HEPES buffer 50 mM pH 7.0 + 100 µL sensor 5 µM, shaking for 3 min. Inset: Zoom for fluorescence intensity between 0 and 10

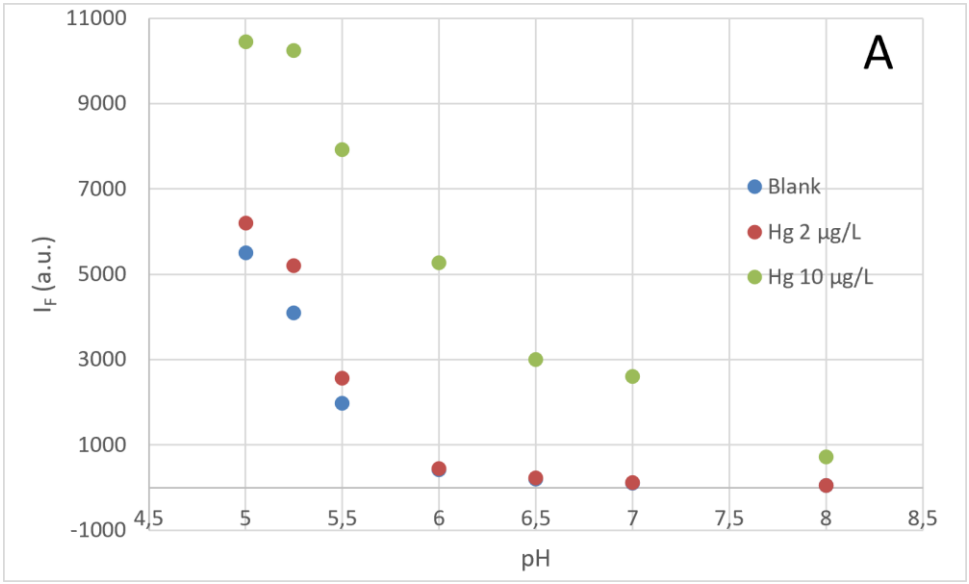


397

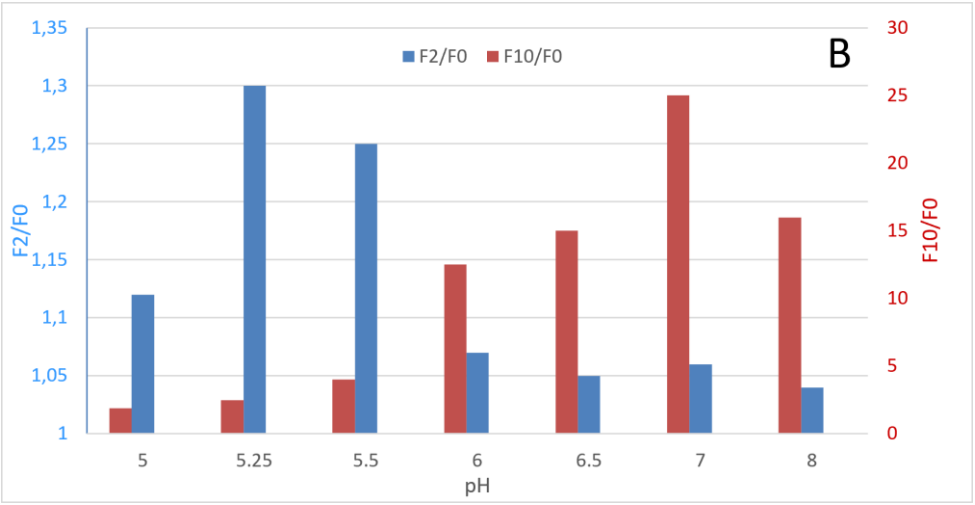


398

399 **Figure 3.** Comparison of the response of **S1** with two standard solutions, depending on the
400 buffer. Microplate protocol. Buffer: Acetic acid 50 mM for pH 5-5.5; MES 50 mM for pH 6-
401 6.5; MOPS 50 mM for pH 7-8. (A) Fluorescence intensities; (B) Ratio of fluorescence
402 intensities between standard solutions and blank (F2/F0: ratio Hg 2 µg.$L^{-1}$/blank; F10/F0: ratio
403 Hg 10 µg.$L^{-1}$/blank)

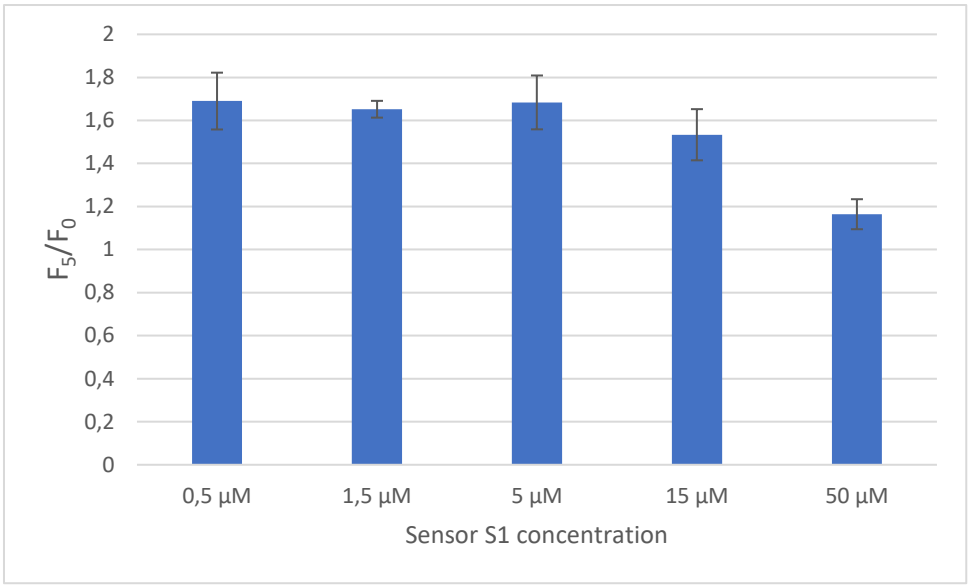


404

405 **Figure 4.** Influence of the sensor **S1** concentration on the fluorescence response. Microplate
406 protocol. Sensor concentration is the concentration in the 25 µL of sensor added to the sample.
407 Buffer: Acetic acid 50 mM pH 5.25. $F_5/F_0$ is the ratio between the fluorescence response of a 5
408 $\mu g.L^{-1}$ standard solution and the blank

409

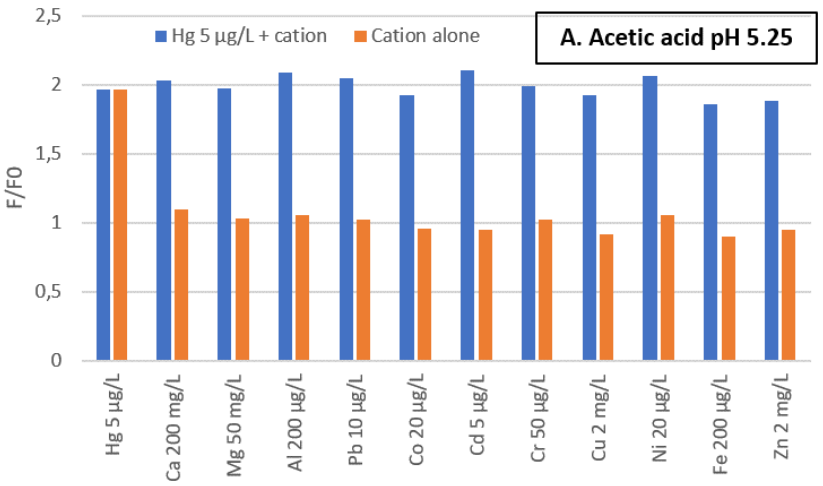


410

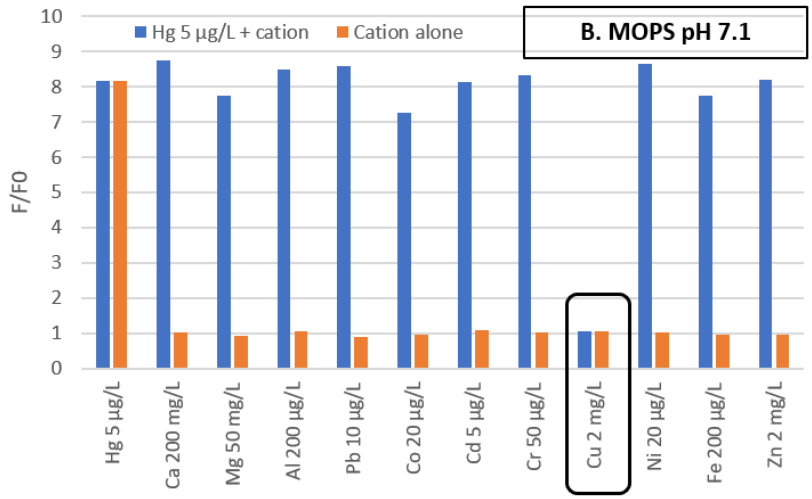


411 **Figure 5.** Selectivity study with sensor **S1**. A. Buffer: Acetic acid 50 mM pH 5.25. B: Buffer:
412 MOPS 50 mM pH 7.1. Microplate protocol, F/F0 is the ratio between the fluorescence response
413 of the metal ions solution and the blank

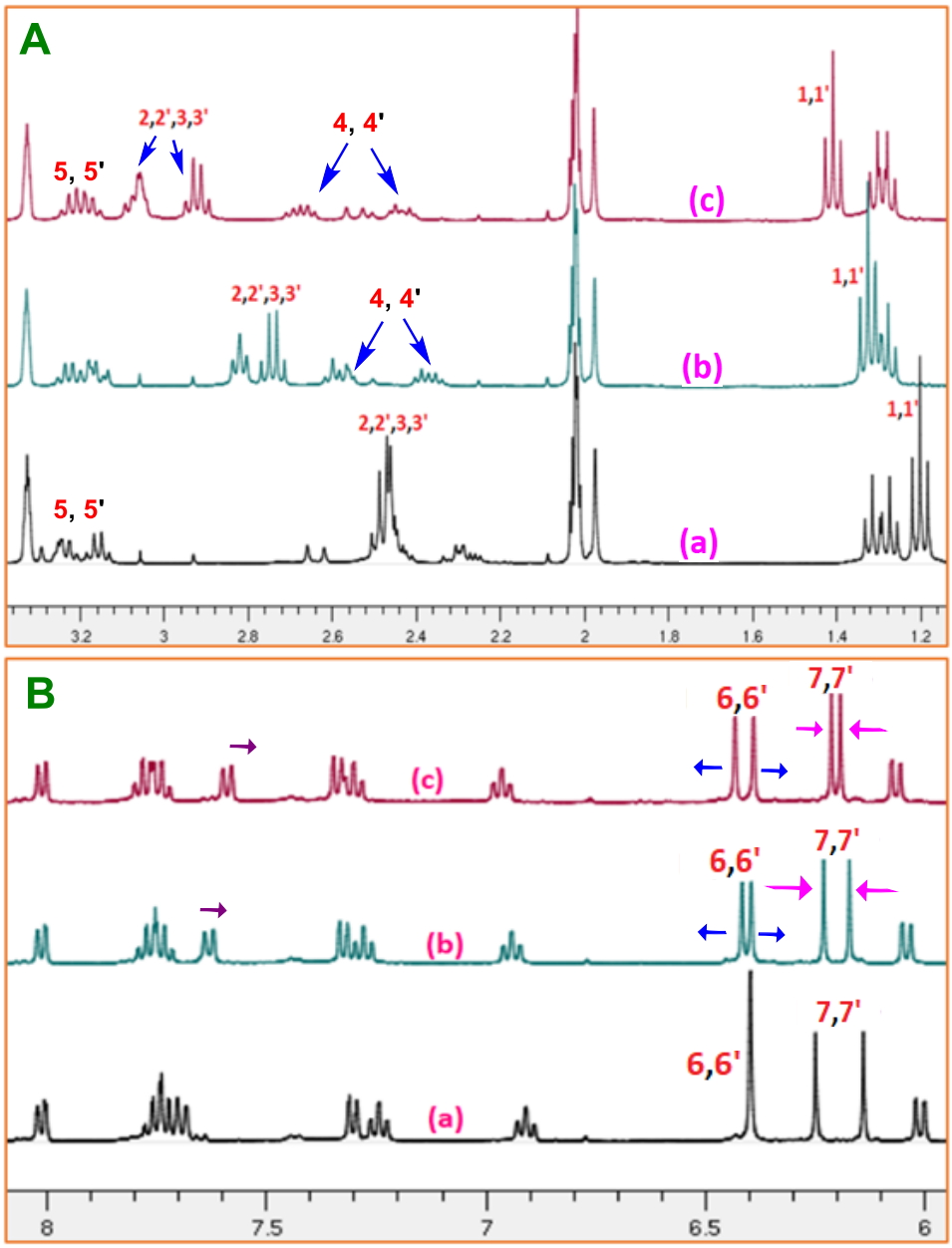


414

415 Figure 6. $^{1}$H-NMR titration of Sensor **S1** (10.0 mM) with $Hg^{2+}$ in $CD_3CN$ and $CD_3OD$ (1:1).

416 (a) Sensor **S1** only; (b) Sensor **S1** + 0.5 equiv of $Hg^{2+}$ and (c) Sensor **S1** + 1.00 equiv of $Hg^{2+}$

417

418

419

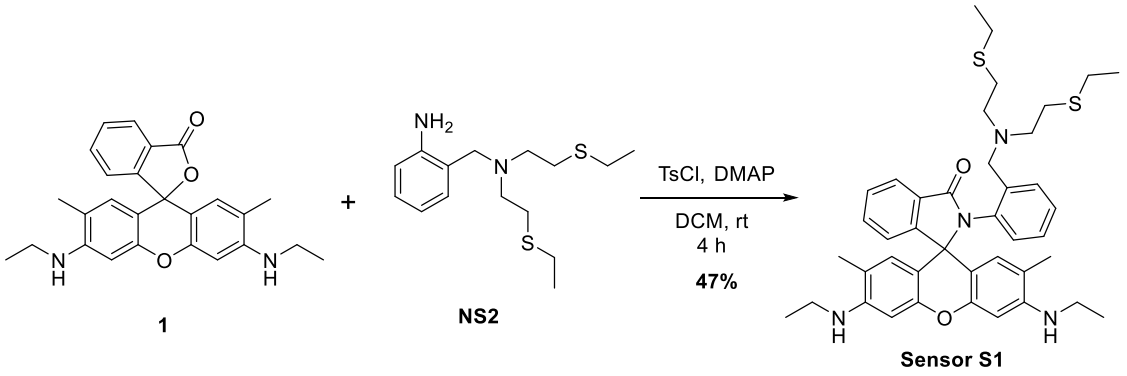


420

421 **Scheme 1**. Synthesis of Sensor **S1**

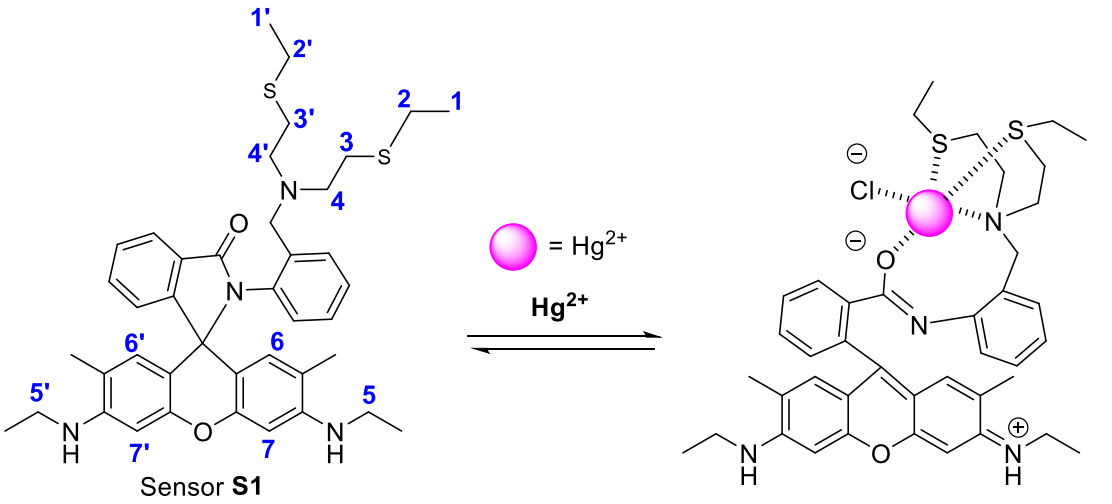


422 **HRMS (ES+): $[M+H]^+$ = 695.3761** **HRMS (ES+): $[M+Hg+Cl]^+$ = 931.3174**

423 **Scheme 2**. Proposed mode of complexation of Sensor **S1** with $Hg^{2+}$

424

425

426

427

428